the generative potential of resinite.

3. Pyrolysis results for resinite vary depending on the technique used. Hydrous pyrolysis more closely defines the temperature at which liquid hydrocarbon generation occurs and the type of products generated.

Acknowledgment. We wish to thank Chevron Oil Field Research Co. for support of this work and permission to publish. Appreciation is extended to P. C. Henshaw, S. R. Jacobson, D. A. Jeffrey, and P. Sundararaman for critical review of this manuscript.

Characterization of Arsenic in Oil Shale and Oil Shale Derivatives by X-ray Absorption Spectroscopy§

S. P. Cramer,* M. Siskin,† L. D. Brown,‡ and G. N. George†

Schlumberger-Doll Research, Old Quarry Road, Ridgefield, Connecticut 06877, and Exxon Research and Engineering Company, Route 22 East, Annandale, New Jersey 07830, and P.O. Box 4255, Baytown, Texas 77520

Received June 12, 1987. Revised Manuscript Received September 29, 1987

X-ray absorption spectroscopy using synchrotron radiation is ideally suited for in situ characterization of trace elements down to the 1 ppm level. With this technique, the chemical nature of the arsenic species in oil shales and derivatives was investigated. Model compound studies revealed that the arsenic absorption edge is sensitive to the oxidation state and covalency of the arsenic environment, shifting from 11 870 eV in metal arsenides and arsenic(III) sulfides to 11 876 eV in arsenic(V) oxides. The arsenic edge of a Green River oil shale (GROS) showed two peaks, consistent with the presence of a metal arsenide or arsenic(III) sulfide as well as an As(V) species. The relative intensities of these two peaks varied in other shales, indicating primarily oxidized arsenic in Rundle Munduran Creek shale to primarily reduced arsenic in Brazilian Irati shale. Concentration of the GROS kerogen resulted in selective removal of the oxidized arsenic species. The merits and potential pitfalls of applying X-ray absorption to complex materials are discussed.

Introduction

Arsenic is present in most oil shales at concentrations of about 10–200 ppm.[1] Because it is a potent catalyst poison, the successful conversion of oil shale into useful liquid fuels is hindered by the presence of this element. The environmental and toxicological problems associated with disposal of guard bed materials and disposal and leaching of spent and combusted shale piles, and in waste water cleanup are significant.[2,3] In order to improve arsenic removal methodology, a good understanding of the nature of the arsenic species present is clearly desirable. Chemical analysis by HPLC and other methods has been applied to oil shale methanol extracts,[4] revealing the presence of arsenate and organoarsonic acids. However, only a small fraction of the arsenic was extracted. On the basis of electron beam[5] and magnetic[6] techniques an association between the bulk of the arsenic and iron sulfide minerals was proposed. Recently, a combined SEM-EDS and X-ray powder diffraction study has revealed the presence of skutterudite $(Co,Fe,Ni)As_3$ and safflorite $(Co,Fe)As_2$ particles.[7] However, quantitation and characterization of diffuse or noncrystalline arsenic is impossible by this method. A complementary technique that is ideally suited for in situ analyses of arsenic-containing materials is X-ray absorption spectroscopy.[8]

X-ray absorption spectroscopy is ideally suited for characterization of the arsenic in oil shale and related materials. With synchrotron radiation sources and X-ray fluorescence detection,[9] the sensitivity is such that concentration levels below 10 ppm can be studied. The edge region, sometimes referred to as XANES or X-ray absorption near edge structure, is sensitive to the absorbing atom oxidation state, site symmetry and ligand covalency.[10]

* To whom correspondence should be addressed at Schlumberger-Doll Research.

§ Presented at the Symposium on Advances in Oil Shale Chemistry, 193rd National Meeting of the American Chemical Society, Denver, CO, April 5–10, 1987.

† Exxon Research and Engineering Co., Annandale, NJ.

‡ Exxon Research and Engineering Co., Baytown, TX.

(1) *Geochemistry and Chemistry of Oil Shales*; Miknis, F. P.; McKay J. F. Eds.; ACS Symposium Series 230; American Chemical Society: Washington, DC, 1983.

(2) Nevens, T. D.; Culbertson, W. J., Jr.; Wallace, J. R.; Taylor, G. C.; Jovanovich, A. P.; Prien, C. H., U.S. DOE Report COO-5107-1, July 1979.

(3) Gurley, L. B.; Tobey, R. A.; Valdez, J. G.; Halleck, M. S.; Bahrman, S. *Sci. Total Environ.* **1983**, *28*, 415.

(4) (a) Fish, R. H. In *Geochemistry and Chemistry of Oil Shales*; Miknis, F. P.; McKay, J. F., Eds.; ACS Symposium Series 230; American Chemical Society: Washington, DC, 1983; pp 423–432. (b) Fish, R. H.; Tannous, R. S.; Walker, W.; Weiss, C. S.; Brinckman, F. E. *J. Chem. Soc. Chem. Commun.* **1983**, 490.

(5) Desborough, G. A.; Pitman, J. K.; Huffman, C., Jr. *Chem. Geol.* **1976**, *17*, 13.

(6) Jeong, K. M.; Montagna, *Prepr. Pap.—Am. Chem. Soc. Div. Fuel Chem.* **1984**, *29*(3), 307.

(7) Jaganathan, J.; Mohan, M. S.; Zingaro, R. A. *Fuel* **1986**, *65*, 266.

(8) (a) *Extended X-Ray Absorption Fine Structure*, Konigsberger, D.; Prins, R., Eds.; Plenum: New York, 1987. (b) *EXAFS and Near Edge Structure III*; Hodgson, K. O., Hedman, B., Penner-Hahn, J. E., Eds.; Springer-Verlag: West Berlin, 1984.

(9) Cramer, S. P.; Scott, R. A. *Rev. Sci. Instrum.* **1981**, *52*, 395–399.

(10) Bianconi, A. In *EXAFS and Near Edge Structure*; Bianconi, A., Incoccia, L., Stipcich, S., Eds.; Springer-Verlag: West Berlin, 1983; pp 118–129.

0887-0624/88/2502-0175$01.50/0

The extended X-ray absorption fine structure or EXAFS[8] can reveal the type, number, and distances of neighboring atoms. The combination of both regions can yield a great deal of information about trace elements in sediments, source rocks, and fuels, and the technique has already been applied to vanadium in asphaltenes[11] as well as sulfur and other elements in coal.[12]

Experimental Section

Sample Preparation. The model compounds As_2S_3, As_2O_3, $As(C_6H_5)_3$, and $As(C_6H_5)_4Cl{\cdot}H_2O$ were obtained from Aldrich Chemical Co. $FeAsO_4$, FeAsS, and $FeAs_2$ were purchased from Varlacoid Chemical Co. $(C_6H_5)AsO(OH)_2$ was bought from Alfa Chemical Co., NiAs from ICN Pharmaceuticals, and $(CH_3)_2AsO(OH)$ from Sigma Chemical Co. A 30-μm sputtered arsenic film was provided by Dr. John Keene of the Energy Conversion Devices Corp., Troy, MI. The sample of $(CN_3H_6)_2[(CH_3)_2AsMo_4O_{15}H]{\cdot}H_2O$ was synthesized by the literature method,[13] as was the $(C_5NH_6)_2[Mo_2(HAsO_4)_2]$ standard.[14] Skutterudite and safflorite were obtained from Dr. Ralph A. Zingaro of Texas A & M University.

Green River Formation shale containing 72 ppm As was obtained from the Colony Mine in Parachute Creek, CO, and then crushed and ground to −100 mesh. Other shales were obtained from the Shale Library at the Exxon Baytown Research and Development Laboratories. Kerogen concentrate was prepared by HCl/HF digestion at 20 °C (180 ppm of As). A poisoned Ni–Mo hydrotreating catalyst was obtained from the Exxon Baton Rouge Research and Development Labs (1.08 wt % As). The source of the spent shale was the Baytown Research and Development Labs Process Shale Unit (61.8 ppm of As). Elemental analyses for arsenic were carried out by General Activation Laboratories, Inc., San Diego, CA.

Data Collection and Analysis. The EXAFS spectra were recorded and analyzed by previously described procedures.[15-18] The spectra were fit according to the following functional form:

$$\chi(k) = \sum_b \frac{N_b A_{ab}(k)}{kR_{ab}^2} e^{-2\sigma_{ab}^2 k^2} \sin\,[2kR_{ab} + \alpha_{ab}(k)] \qquad (1)$$

where N_b is the number of type b atoms at distance R_{ab} and mean square deviation σ_{ab}^2 from the arsenic central atom a. $A_{ab}(k)$ and $\alpha_{ab}(k)$ are total amplitude and phase shift functions, respectively, and k is the magnitude of the photoelectron wave vector. An E_0 of 11878 eV was used to define k in all spectra.

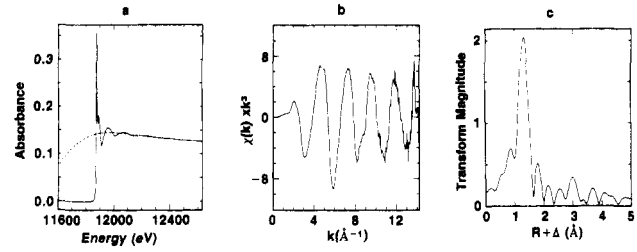

Figure 1. General features of arsenic K X-ray absorption edge spectra, illustrated using data for $FeAsO_4$. (a) The overall spectrum has a sharp spike at the edge, followed by broad oscillations (EXAFS), which can be better seen by removing a smooth curve (dashed line). (b) The EXAFS oscillations are generally plotted vs. photoelectron wave number $k = 0.26(E - E_0)$, where E is the photon energy and E_0 is the core electron binding energy. Since the oscillations damp out rapidly with increasing energy, they are often multiplied by k^3 to reveal the high-energy structure. (c) The Fourier transform of the EXAFS oscillations has major peaks that correspond to interatomic distances, shifted from the true distance by about 0.4 Å because of the k-dependent phase shift (see eq 1). In this case the dominant peak represents the As–O interaction.

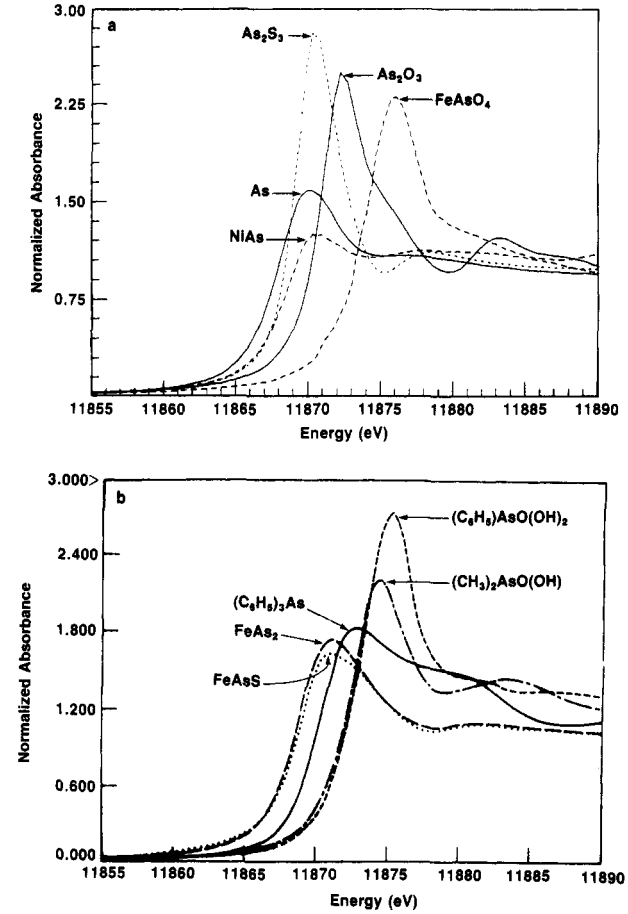

Figure 2. (a) Arsenic K absorption edge region for standard compounds with homogeneous first coordination spheres: short dashes, As_2S_3; solid line with lower energy peak, pure As; solid line with higher energy peak, As_2O_3; dashed line with lower energy peak, NiAs; dashed line with higher energy peak, $FeAsO_4$. The spectra were normalized to the same absorbance at 12 100 eV. (b) Arsenic K absorption edge region for additional standard compounds: long dashes, $FeAs_2$; dotted line, FeAsS; solid line, $(C_6H_5)_3As$; short dashes, $(C_6H_5)AsO(OH)_2$; dash dot, $(CH_3)_2AsO(OH)$.

From (1), the total phase shift $\alpha_{ab}(k)$ is determined by using the EXAFS of model compounds with known interatomic distances R_{ab}.[16,17] However, the amplitude function $A_{ab}(k)$ can only be determined empirically if both the number of atom neighbors N_b and the mean square distance deviation σ_{ab}^2 are known.[17,18]

(11) Goulon, J.; Retournard, A.; Friant, P.; Goulon-Ginet, C.; Berthe, C.; Muller, J.; Poncet, J.; Guilard, R.; Escalier, J.; Ness, B. *J. Chem. Soc., Dalton Trans.* **1984**, 1095–1103.

(12) Spiro, C. L.; Wong, J.; Lytle, F. W.; Maylotte, D. H.; Greegor, R. B.; Lamson, S. H. *Science (Washington, D.C.)* **1984**, *226*, 48–50.

(13) Barkigia, K. M.; Rajovic-Blazer, L. M.; Pope, M. T.; Prince, E.; Quicksall, C. O. *Inorg. Chem.* **1980**, *19*, 2531–2537.

(14) Ribas, J.; Poilblanc, R.; Sourisseau, C.; Solans, X.; Brianso, J. L.; Miravitlles, C. *Transition Met. Chem. (Weinheim, Ger.)* **1983**, *8*, 244–250.

(15) The model compound spectra were recorded in transmission mode at the Stanford Synchrotron Radiation Laboratory, either on bending magnet beam lines I-5 or II-3 during 3-GeV dedicated operation or on wiggler beam line VII-3 during parasitic running at 1.85 GeV. The shale and shale-derived samples were investigated in fluorescence mode by using Ge filters[9] on beam lines VII-3 or VI-2 during 3-GeV dedicated operation. Adequate edge spectra were obtained on 10 ppm samples in about 1 h on the latter beam line. Si(2,2,0) monochromators were used in all cases and were calibrated by using 11 868 eV for the elemental As edge first inflection point.

(16) Cramer, S. P.; Hodgson, K. O.; Stiefel, E. I.; Newton, W. E. *J. Am. Chem. Soc.* **1978**, *100*, 2748–2761.

(17) Cramer, S. P. *EXAFS for Inorganic Systems*; Garner, C. D., Hasnain, S. S., Eds.; Daresbury Laboratory: Daresbury, England, 1981; pp 47–50.

(18) Cramer, S. P.; Wahl, R.; Rajagopalan, K. V. *J. Am. Chem. Soc.* **1981**, *103*, 7721–7727.

Table I. Parameters for As-X Amplitude and Phase Shift Functions $A(k) = c_0 e^{c_1 k + c_2 k^2} k^{c_3}$ and $\alpha(k) = a_0 + a_1 k + a_2 k^2 + a_3 k^{-1}$

interaction	c_0	c_1	c_2	c_3	a_0	a_1	a_2	a_3
As–C	0.056 080	−1.148 5	0.024 343	3.8270	−3.5636	−0.416 86	−0.002 760 0	13.616
As–O	0.310 66	−1.081 5	0.026 773	2.7651	−5.4269	−0.876 91	0.013 674	5.9102
As–S	0.118 08	−0.838 75	0.013 841	3.1523	3.7356	−0.791 17	0.013 123	10.352
As–Mo	0.001 554 5	0.074 236	−0.016 443	2.5300	16.070	−1.032 8	0.006 141 8	−15.815

Although σ^2 is difficult to calculate for all but the simplest molecules, an iterative "bootstrap" procedure can be used to estimate appropriate values.[19]

Results

The overall structure of arsenic X-ray absorption is illustrated in Figure 1. The spectra contain a sharp X-ray absorption edge region, followed by broad oscillations (EXAFS), which extracted and Fourier transformed yield something like a radial distribution function. Since XANES and EXAFS use different analyses, they are best discussed separately.

Standard Compound Edges. Arsenic edges are extremely sensitive both to the arsenic oxidation state and to the nature of the surrounding ligands, as illustrated in Figure 2. A 6-eV chemical shift is evident between elemental arsenic and $FeAsO_4$. The fact that sulfur ligands or a lower oxidation state shift the absorption edge to lower energies has been observed previously for molybdenum[22,23] and in numerous other cases.[10] In fact, chemical shifts in arsenic edges were observed as far back as 1949.[24]

Three distinct regions can be defined which are of relevance for shale-related materials. The low-energy region, in the vicinity of 11 870–11 871 eV, encompasses samples as diverse as elemental arsenic, NiAs, and As_2S_3. The intermediate range, near 11 872.5 eV, corresponds to As(III) compounds with carbon and/or oxygen ligands. Finally, the high-energy range, 11 875–11 876 eV, also reflects an environment with carbon and/or oxygen ligands, but with As in the As(V) oxidation state.

The initial sharp rise in absorption at the arsenic edge corresponds approximately to a 1s → 4p transition. Not only does this edge peak change in position but also the intensity of the edge transition varies more than twofold. For example, the intensity is dramatically higher in the case of As_2S_3 than it is in elemental As or NiAs, even though the edge position is nearly the same. Similar variations in edge intensities in GeH_4 and $GeCl_4$ have been reported and analyzed by Natoli et al.,[25] who ascribe the

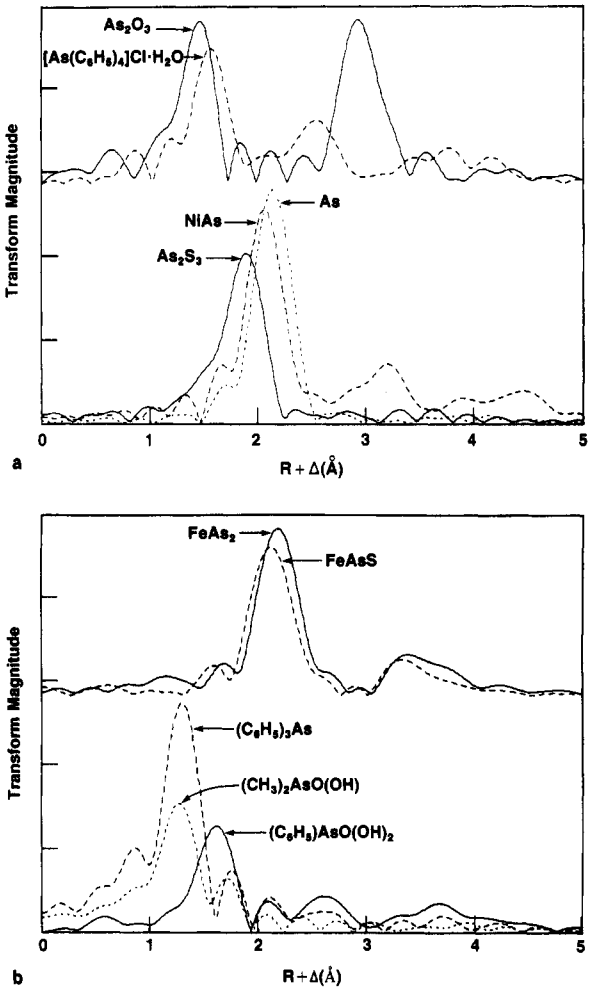

Figure 3. (a) EXAFS Fourier transforms for standard compounds with homogeneous first coordination spheres: top (solid line), As_2O_3; top (dashed line), $[As(C_6H_5)_4]\cdot H_2O$; bottom (solid line), amorphous As_2S_3; bottom (long dashed line), NiAs; bottom (short dashed line), pure As. Transform range: k = 4–16 Å^{-1}, k^3 weighting. (b) EXAFS Fourier transforms for additional standard compounds: top (solid line), $FeAs_2$; top (dashed line), FeAsS; bottom (solid line), $(C_6H_5)AsO(OH)_2$; bottom (dashed line), $(C_6H_5)_3As$; bottom (short dashed line), $(CH_3)_2AsO(OH)$. Transform range: k = 4–15 Å^{-1}, k^3 weighting.

(19) For the present work an initial fit to the standard compound spectra using the functional form of (1), with σ^2 set to zero, was done by optimizing the parameters in the phase shift and amplitude functions:

$$A(k) = c_0 e^{(c_1 k + c_2 k^2)} k^{c_3}$$

$$\alpha(k) = a_0 + a_1 k + a_2 k^2 + a_3 k^{-1}$$

With the phase shift determined by this procedure, a second refinement was done, with

$$A(k) = S_{ab} |f_b(\pi,k)|$$

where S_{ab} is a scale factor and $|f_b(\pi,k)|$ is the appropriate backscattering amplitude from the tables of Teo and Lee.[20] In this second refinement both the scale factor and σ^2 were allowed to vary. The σ^2 value thus obtained was then used to correct the parameterized $A(k)$ for thermal motion and other disorder in the standard compound by adjustment of parameter c_2. Finally, the phase shift function was adjusted by integral multiples of 2π to the range, yielding an asymptotic approach to the tabulated theoretical values. Although the methodology is quite different from the FAB method described by Teo and co-workers,[21] this "bootstrap" procedure has a functionally equivalent net result. In both cases, one ultimately obtains phase shift and amplitude functions for which the appropriate scale factors and E_0 shifts have been derived by the use of model compounds. This permits curve-fitting unknown spectra without the use of scale factors and E_0 shifts as adjustable parameters, which is otherwise required when the purely theoretical functions are used alone.

(20) Teo, B. K.; Lee, P. A. *J. Am. Chem. Soc.* **1979**, *101*, 2815–2832.

(21) Teo, B. K.; Antonio, M. R.; Averill, B. A. *J. Am. Chem. Soc.* **1983**, *105*, 3751–3762.

(22) Cramer, S. P.; Hodgson, K. O.; Gillum, W. O.; Mortenson, L. E. *J. Am. Chem. Soc.* **1978**, *100*, 3814–3819.

(23) Cramer, S. P.; Eidem, P. K.; Paffett, M. T.; Winkler, J. R.; Dori, A.; Gray, H. B. *J. Am. Chem. Soc.* **1983**, *105*, 799–802.

(24) Cauchois, Y.; Mott, N. F. *Philos. Mag.* **1949**, *40*, 1260–1269. Although these authors reported the edge of NiAs at lower energy than that of elemental As, we have observed a different shift.

(25) Natoli, C. R.; Misemer, D. K.; Doniach, S.; Kutzler, F. W. *Phys. Rev. A* **1980**, *22*, 1104–1108.

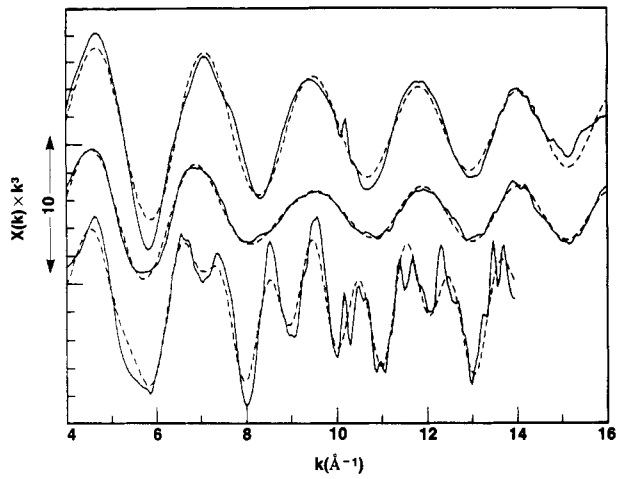

Figure 4. Curve-fitting analysis of some model compound spectra. The solid line is smoothed experimental data, and the dashed line is the calculated EXAFS from curve fitting: top, $(C_6H_5)AsO(OH)_2$; middle, $(CH_3)_2As(O)OH$; bottom, aqueous solution containing $[(CH_3)_2AsMo_4O_{15}H]^{2-}$.

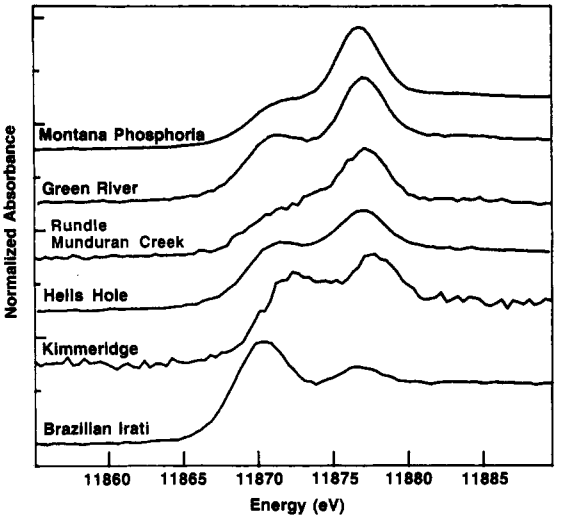

Figure 5. Arsenic K absorption edges for a variety of oil shales: top to bottom, Montana Phosphoria shale, Green River shale, Rundle Munduran Creek shale, Hells Hole shale, Kimmeridge shale, and Brazilian Irati shale.

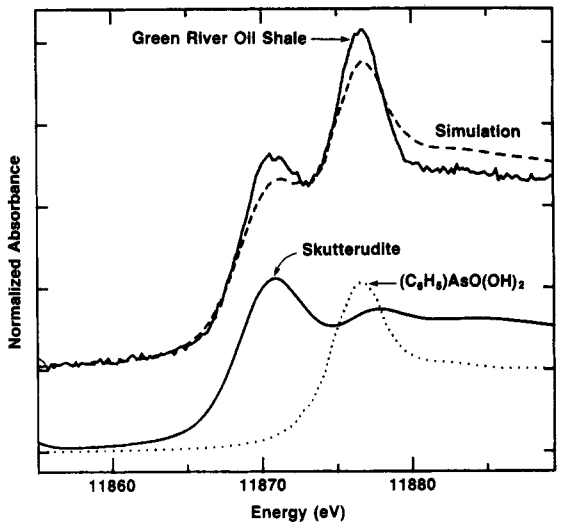

Figure 6. Simulation of Green River oil shale arsenic K absorption edge as the sum of skutterudite and phenylarsonic acid standards. The upper pair of traces shows the Green River oil shale edge (—) vs. a simulation (- - -) composed of 0.69 skutterudite and 0.39 phenylarsonic acid edges. The lower pair of traces shows the two standard edges, skutterudite (—) and phenylarsonic acid (- - -). The standard compound data were shifted in energy slightly to align the peaks with those of the oil shale.

differences to the relative backscattering power of the neighboring atoms. However, the amplitude of the edge resonance is not a simple function of the atomic number of the arsenic neighbors.

A qualitative interpretation in terms of 4p vacancies makes sense for these edges. The electronic configuration of As(V) is $[Ar]3d^{10}4s^04p^0$. Because of the empty 4p shell, it exhibits a strong 1s → 4p transition at the absorption edge. Reduction to As(III) fills only the 4s subshell and hence does not affect the edge intensity. Further reduction to As(0) or As^{2-} begins filling the 4p shell and leads to a dramatic loss in intensity. A more quantitative interpretation requires calculations on the local electronic structure that are beyond the scope of this work.

Standard Compound EXAFS Fourier Transforms. The EXAFS Fourier transforms of the model compounds used for extraction of phase shift and amplitude functions are shown in Figure 3a, and the functions derived from the EXAFS spectra are included as Table I. Transforms for several additional arsenic compounds are illustrated in Figure 3b. In both figures, the major peaks correspond to sets of atoms whose distances from arsenic is approximately 0.4 Å longer than that observed in the transform itself. This shift from the true distance can be related to the average slope of the phase shift $\alpha(k)$.

The Fourier transform is a useful qualitative tool for displaying the chief characteristics of the As coordination sphere. Even without curve fitting, the first coordination sphere features can qualitatively be interpreted because of the fact that As–S bonds tend to be significantly longer than As–O or As–C bonds. As–M interactions, where M is a metal such as Fe or Ni, occur at even longer distances. Finally, second coordination sphere features that are particularly enhanced are As–O–As and As–M–As interactions. Thus, a predominance of short distance features in the transform indicates As–C or As–O coordination, whereas longer distances peaks suggest a As–S or As–M environment.

The only unusual result from analysis of the standard spectra is the lack of an As–As second-shell feature in the As_2S_3 transform. Subsequent X-ray powder diffraction analysis showed the material to be amorphous.

Standard Compound EXAFS Curve Fitting. Better quantitation of EXAFS spectra can be achieved by curve-fitting analysis using the functions of Table I. Fits on arsenic compounds of known structure are illustrated in Figure 4. In simple structures with two or three As–X interactions, distances are calculated with 1% accuracy.

Curve-fitting analysis is full of pitfalls when the number of different types of interactions grows beyond three or four. This is especially true when the analysis is more concerned with bond numbers than bond lengths. Since the shale-related samples examined in this study all contain a mixture of arsenic species, a quantitative analysis of the raw whale EXAFS has not been completed.

Oil Shale Absorption Edge Survey. The arsenic absorption edges for a variety of oil shales are compared in Figure 5. In all cases two distinct features are observed, one peak in the low-energy region characteristic of reduced arsenic and a second high-energy peak characteristic of As(V). Thus, it appears there are at least two classes or arsenic compounds in these materials, and the variation in intensities shows that the relative amounts do change. Since the edge amplitudes are not directly related to concentration, especially for the reduced species, it is

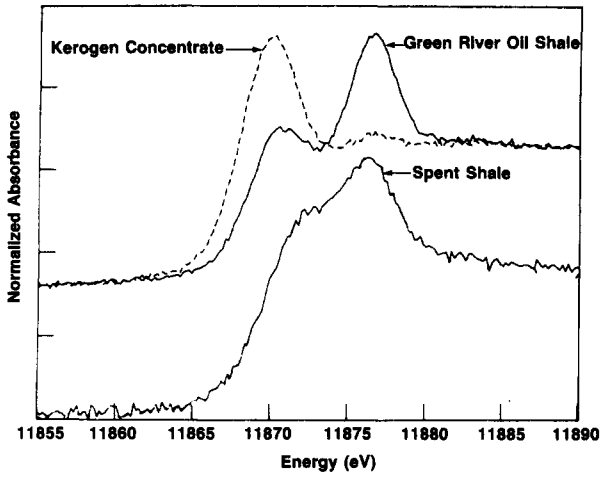

Figure 7. Arsenic K absorption edges for Green River oil shale and derivatives: top (---) untreated shale, (—) kerogen concentrate; bottom, spent shale (—).

difficult to quantitate the relative amounts. However, if one assumes a mixture of skutterudite and phenylarsonic acid, then the edge of Green River oil shale can be simulated as the sum of a 1.8:1 mixture of these species, as shown in Figure 6.

On the basis of acid extraction analyses, scanning electron microscopy, and X-ray diffraction, Zingaro and coworkers concluded that 65% of the arsenic in Green River oil shale is present as skutterudite and safflorite.[7] Our results are consistent with the presence of such minerals, but they also indicate the presence of oxidized forms of arsenic in variable amounts. The oxidized species are the dominant component of the Montana Phosphoria shale sample, while they are nearly absent from the Brazilian Irati sample. In separate experiments, we have observed variability in the relative amounts of oxidized and reduced species in different Green River oil shale samples and also from one layer to another on a millimeter scale within the same piece of Green River shale.

Oil Shale Derivatives. The strikingly different absorption edge regions for Green River oil shale and a kerogen concentrate are shown in Figure 7. The As(V) feature is smaller in the kerogen concentrate edge, and the spectrum is dominated by a low-energy peak. This is consistent with the hypothesis that oxidized, As(V) compounds are removed during the kerogen concentration procedure. Also shown in Figure 7 is the arsenic absorption edge for a spent Green River oil shale, which exhibits a distinct As(V) peak, as well as a shoulder that may represent a mix of reduced species.

The EXAFS Fourier transforms in Figure 8 Green River oil shale and kerogen concentrate are quite different. The raw shale data is dominated by a short distance feature, indicating primarily As–C or As–O coordination. Curve-fitting analysis yields an average As–C,O distance of 1.74 Å, nearly identical with the 1.73-Å As–OH distance in phenylarsonic acid. There is also a significant longer distance peak in the region characteristics of As–S or As–M coordination. Curve fitting this feature as an As–Fe interaction yields an As–Fe distance of 2.35 Å, close to the 2.33-Å As–metal distance in skutterudite. The observation by EXAFS of at least two types of arsenic ligation in shale is thus consistent with the edge results.

The kerogen concentrate sample has an EXAFS Fourier transform dominated by a peak centered at $R + \Delta \simeq 1.95$ Å. Although the peak position is slightly shifted from the corresponding peak in the raw shale Fourier transform, the shift in the latter appears to be a transform artifact caused

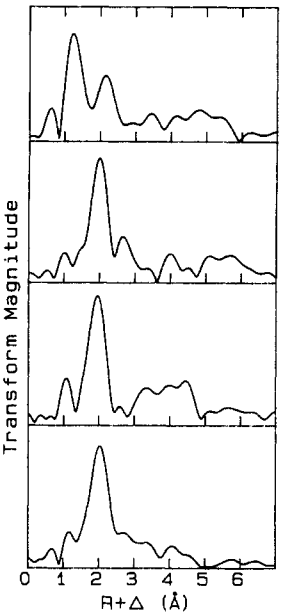

Figure 8. EXAFS Fourier transforms for (top to bottom) raw Green River oil shale, kerogen concentrate, Brazilian Irati shale, and skutterudite. Transform range: k = 0–10 Å^{-1}, k^3 weighting.

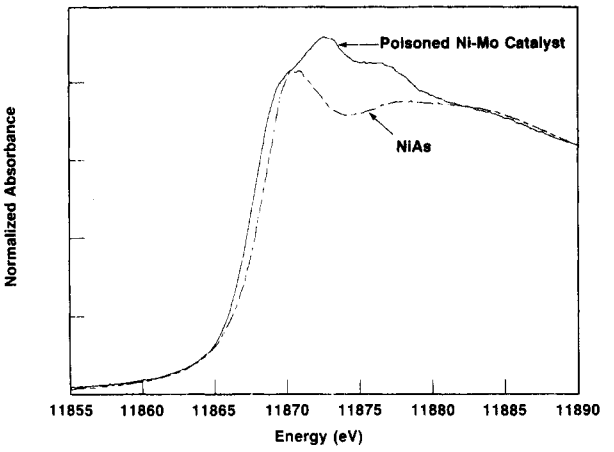

Figure 9. Arsenic absorption edge region for poisoned Ni–Mo catalyst (—) and NiAs (---).

by overlapping components. Curve fitting the kerogen concentrate EXAFS yields an As–metal true distance of 2.34 ± 0.03 Å, the same within experimental error as in the raw shale. This dominant long-distance feature suggests primarily As–M and/or As–S coordination, again in accord with the edge result.

Figure 8 also includes the EXAFS Fourier transforms for Brazilian Irati oil shale and a sample of skutterudite. As with the absorption edge region, the Irati shale EXAFS indicates a much larger reduced arsenic fraction than in the Green River sample.

Poisoned Catalyst. The arsenic absorption edge for a poisoned Ni–Mo hydrotreating catalyst is compared with the edge of nickel arsenide in Figure 9. Peaks assignable to NiAs have been observed in arsenic-poisoned catalysts.[26] Although there is some similarity of features in both spectra, the poisoned catalyst edge has additional structure not present in the NiAs spectrum, and it is clearly not pure NiAs with a 1:1 stoichiometry. Examination of the Fourier transforms, Figure 10, again shows that the poisoned catalyst and NiAs are similar, but only about half of the arsenic could be accounted for as NiAs.

(26) Brown, L. D., unpublished observation.

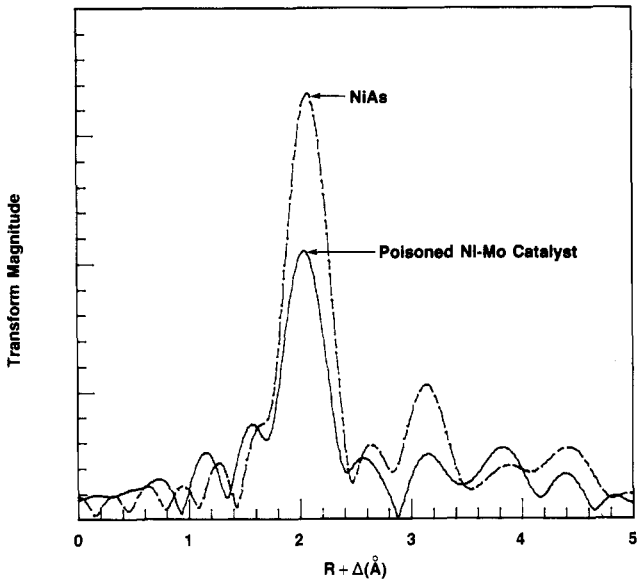

Figure 10. EXAFS Fourier transforms for poisoned Ni-Mo catalyst (—) and NiAs (- - -). Transform range: k = 4–14 Å^{-1}, k^3 weighting.

Summary and Conclusions

Because it is present in relatively low concentrations, 10–200 ppm, the nature of arsenic in oil shale has been difficult to study. The current results are consistent with the presence of at least two classes of arsenic. The XANES and EXAFS suggest the presence of both arsenic(V) species in oxygen and/or carbon environments, as well as more reduced species with As–S or As–M ligation. Furthermore, the relative amounts of these two types of arsenic vary between different types of oil shale.

One surprising result of the current work was the profound difference between arsenic in the kerogen concentrate and the raw shale. It appears that treatment with HCl and HF and copious washing with distilled water removes the As(V)–(C,O) species, which include arsenate salts. Since mineral forms of arsenic such as skutterudite and safflorite, as well as arsenic sulfides and iron arsenic sulfide, are insoluble in water and acid, it is reasonable that a chemical separation of arsenic species during the kerogen concentration procedure occurs.

The upgrading of raw shale oil to synthetic crude requires removal of organic nitrogen by hydrodenitrogenation (HDN) over active metal catalysts. Curtin[27] has shown that the HDN activity of a commercial nickel–molybdenum hydrotreating catalyst rapidly declined due to the presence of arsenic in the oil. Although it has been speculated[3] that NiAs forms under these conditions, the results on the Ni–Mo catalyst suggest that a more complex reaction takes place. Additional species including organic As(III) and As(V) compounds may be present.

The presence of multiple and variable As species in oil shales raises questions about the origin and possible diagenesis of arsenic in these materials. The bioaccumulation of arsenic in the form of arsenobetaine by algae and other organisms is well-known.[28] However, it is unclear whether all arsenic in shales passes through living organisms. The events involved in arsenic mineral formation also remain unclear.

Because it can examine arsenic and other trace elements at ppm levels without additional sample treatment, X-ray absorption spectroscopy should be a useful tool for these and other geochemical questions.

Registry No. As, 7440-38-2.

(27) Curtin, D. J.; Dearth, D. J.; Everitt, G. L.; Grosboll, M. P.; Myers, G. A. *Prepr. Pap.—Am. Chem. Soc., Div. Fuel Chem.* **1978**, *23*(4), 18.
(28) Shiomi, K.; Shinagawa, A.; Igarashi, T.; Yamanaka, H.; Kikuchi, T. *Experientia* **1984**, 1427–1428.